The principles of cascading power limits in small, fast biological and engineered systems

Mark Ilton,[1*] M. Saad Bhamla,[2*] Xiaotian Ma,[3*] Suzanne M. Cox,[4*] Yongjin Kim,[1] Je-sung Koh,[5] Deepak Krishnamurthy,[2] Chi-Yun Kuo,[4] Fatma Zeynep Temel,[5] Alfred J. Crosby,[1] Manu Prakash,[2] Gregory Sutton,[6] Robert J. Wood,[5] Emanuel Azizi,[7†] Sarah Bergbreiter,[3†] and S. N. Patek.[4†]

[1]Department of Polymer Science and Engineering, University of Massachusetts Amherst, Amherst, MA 01003, USA

[2]Department of Bioengineering, Stanford University, Stanford, CA 94305, USA

[3]Department of Mechanical Engineering and Institute for Systems Research, University of Maryland, College Park, College Park, MD 20742, USA

[4]Department of Biology, Duke University, Durham, NC 27708, USA

[5]School of Engineering and Applied Sciences and Wyss Institute for Biologically Inspired Engineering, Harvard University, Cambridge, MA 02138, USA.

[6]School of Biological Sciences, University of Bristol, Bristol BS8 1TH, UK

[7]Ecology and Evolutionary Biology, University of California Irvine, Irvine, CA, USA

*Co-first authors †Co-last authors

One sentence summary: Disparate worlds of fast biological and engineered movement are unified via a mathematical model, conceptual framework, and literature analysis.

Abstract

Mechanical power limitations emerge from the ~~inextricable,~~ physical trade-off between force and velocity~~. Whether power is measured in launching missiles or running humans,~~ it is impossible to maximize both force and velocity. Many biological systems incorporate power-enhancing mechanisms to great effect, enabling accelerations that exceed bullets and missiles; yet how these mechanisms actually enhance power output is not clear. Here we establish how power enhancement emerges through dynamic coupling of motors, springs, and latches. Power output of motors can be enhanced by springs only under particular conditions and the power dynamics (and limitations) of springs are influenced by their own mass, mechanical properties, and time-dependent behavior. Latch mechanisms mediate potential energy storage and the rate of energy transfer from a spring to a projectile. The integration of mathematical, physical, engineering, and evolutionary approaches illuminates the cascading challenges of power enhancement and their emergent effects in biological and engineered systems.

Introduction

Certain organisms are renowned for their ability to circumvent the force-velocity trade-off of muscle motors through mechanisms of power amplification which can greatly reduce the amount of time required to perform a given amount of work (force × velocity = work/time = power) (1–3). Numerous studies have explored muscular power output and the underlying force-velocity trade-offs (4, 5), as well as the enhanced power output achieved through the use of springs, and often latches (6–11); however, these studies have yet to fully explain the limits of mass-specific power output (power density; W/kg) in these organisms. For example, in many of these systems, the motor does work to store energy in a spring and then the spring solely actuates the power amplified motion. The spring serves as the actuator for the system and, therefore, must operate under its own mass-specific power limits analogous to the motor; however, the power densities of elastic materials are largely unknown for biological and synthetic systems.

Here we probe how non-idealized accessory structures, such as springs and latches, are able to enhance and mediate power output. We apply a modeling approach that is grounded in a simplified power amplification system (Fig. 1), which delineates the limits, integration and scaling of these systems. Our goal is to formulate the fundamental interactions of mechanical power amplification that apply to both engineered and biological systems. We begin by using the model to successively investigate the role of motors, springs, and latches in mechanical power amplification, and briefly review the current understanding of each of these components in the engineering and biological literature. We conclude by examining the connections across the motor, spring, and latch in the context of engineering fabrication and the principles of design revealed through evolutionary trade-offs.

A foundational lesson from archery

Archery illustrates the benefits and limits of power amplification that emerge, as in many biological systems, from the integration of a motor, spring, and latch. Arm muscles serve as the motor that

puts energy into the elastic bow (the spring). Fingers act as latches that resist the elastic energy stored in the bow and determine the timing of energy delivery from the bow to the arrow. The arrow is launched solely by the elastic energy stored in the bow. The addition of a bow to the arm's motor has two distinct benefits. First, the bow decouples the motion of the arm muscles from the arrow's launch, such that the arm muscles need not contract quickly or powerfully; instead, the muscles can contract slowly and forcefully to load a stiff spring. Second, the bow can launch the lightweight arrow without the inertial load of the arm. As a result, the arrow is launched with significantly higher velocity, kinetic energy, and acceleration than if it had been thrown rapidly by the same arm muscles that loaded the bow. Even so, while it is sensible to launch a lightweight arrow with a bow, we would not reach for a bow to launch a heavy stone and would instead throw it directly with our arm muscles. This suggests that the relative size of the projectile should determine whether the bow yields higher launching kinetic energy than possible from the arm alone (12). Optimizing the system would involve tuning the properties of the elastic bow to the force capacity of the arm muscle and the fingers' ability to restrain the bow's release. Just as in archery, the spatial and temporal decoupling of motor and spring, the use of slow and forceful muscle contractions, the tuning of muscle, spring, and latch work capacity, and the reduction of inertial load are hallmarks of biological power-amplified systems (6, 7).

Spring-driven versus motor-driven projectiles

These lessons from archery and their shared characteristics in biology prompted the guiding question ~~of this section~~: *Under which inertial-loading conditions is a projectile best launched by a motor versus a spring?* We constructed a simple mathematical model that consists of an ideal motor, spring, and latch that ~~launched~~ projectiles of varying mass, m. We used a linear force-velocity relation for the motor and held this relationship constant during the simulation (Fig. 1a). We then solved the dynamic equations of motion for a projectile load mass (see supplemental materials for details) launched by either the motor alone (Fig. 1b) or by a spring that was pre-loaded by that same

motor (Fig. 1c). Given our focus on systems that can be used repeatedly over time, we examined engineered motors as opposed to combustion-driven movements that are typically single use (e.g. bullets).

The simulation yielded distinct outcomes for spring-driven versus motor-driven launches that depended on the projectile's mass (Fig. 2). For motor-only actuation, if the projectile mass, m, was low, then the take-off velocity, v_{to}, was limited by the speed of the motor, as seen in the asymptotic approach to $v_{max} = 5\,\mathrm{m/s}$ as m approaches zero. When the projectile mass was high, the take-off velocity was limited by the inertia of the projectile. In the case of spring-driven actuation, take-off velocity was not limited by the motor when the projectile mass was low, and the resulting take-off velocity was much larger than in the motor-driven case.

This analysis highlights a key transition between small masses, which can achieve high velocities through the addition of elastic elements, and large masses, which are constrained by their inertial loads. The addition of a spring is, therefore, most beneficial when the take-off velocity of the projectile is limited by motor velocity. Elastic mechanisms are not particularly effective when the take-off velocity is limited by the inertia of the projectile. However, spring-loaded systems confer a great advantage when a projectile mass is small.

The location of this transition to effective spring actuation depends on the focal kinematic parameter. For example, if the goal is to maximize take-off velocity, the transition occurs at a much smaller projectile mass than if the parameter of interest is take-off duration or maximum power output (Fig. 2). These analyses of the effective integration of motors, springs and projectile masses yield a rich landscape of kinematic performance that can be analyzed in biological systems and ultimately designed into synthetic systems.

Diversity of motors in power-amplified systems

The motors found in biological power-amplified systems maximize force development at the cost of loading velocity and do so at exclusively small inertial loads (Tables 1,2). For example, the surface tension catapults of some fungal spores (ballistospores) use a slowly-developed fluid droplet, which develops over tens of seconds, as their motor and then rapidly release the surface

tension energy of the droplet in less than a microsecond (13, 14). Invertebrates, such as trap-jaw ants and mantis shrimp use long sarcomeres (the contractile units of muscle) to generate slow, but forceful contractions to load the elastic elements that subsequently power their extremely rapid movement (15, 16). Plants, such as Venus flytraps, aquatic bladderworts and fern sporangia utilize non-muscular hydraulic movements (or nastic movements) coupled with elastic instabilities to achieve rapid motion (17–20). For all of these organisms, it often takes orders of magnitude longer to load the system than it does to release the energy; in other words, it takes a long time to store substantial work in an elastic structure and thereby amplify the power output of the underlying motor (21).

Force-velocity trade-offs are ubiquitous in engineered systems and, in many cases, a linear force-velocity trade-off is a good approximation of motor behavior. Engineered power amplified systems are often designed to propel a larger range of inertial loads than in biological systems (Tables 1,2). The majority of engineered systems use DC motors with transmissions designed to generate large torques that slowly load spring elements (22–32). Unlike the biological examples ~~described above~~, the motors are not typically optimized for work density. In comparison to skeletal muscle, the lower power density of some of the motors listed in Table 1 increases the mass at which spring loading is beneficial. Another common actuator choice in the smallest engineered systems ~~is~~ shape memory alloy (SMA), which is chosen for its high specific force and linear actuation (33–35). This high specific force comes with a consequence of low velocities limited by the time required to heat and cool the material above and below its transition temperature. Both of these engineering actuator choices result in long loading times relative to release, similar to their biological counterparts. However, it is important to note that engineered systems are not limited by the power density of muscle. As a consequence, a ~~few~~ engineered jumping systems ~~in~~ Table 2 use combustion, powerful pneumatic actuators, or high power electromagnetic actuators that actuate directly without the use of power amplification mechanisms (30, 31, 36–41).

The power of springs as actuators

Although most of the focus on power amplification has historically revolved around the force-velocity trade-off of motors, the dynamic behavior of springs is the source of power in systems that are exclusively actuated by springs (12). However, springs have typically been characterized in terms of force-displacement curves and defined by geometrical and material properties, leaving open their potential for power enhancement (42, 43). Building on the mathematical model of the previous section, in this section we ask: *What are the implications of spring force-velocity behavior for the generation of power amplification?*

Using the model, we find that the inertia of the spring leads to a force-velocity trade-off for the spring-driven system (Fig. 3), even for the case of the relatively light ($m_s = 0.1$ g) spring used in the previous section. The net force acting on the projectile depends on position and velocity for both the motor-driven (Fig. 3a) and spring-driven (Fig. 3b) systems, which suggests that force-displacement trade-offs should be taken into consideration alongside force-velocity trade-offs for actuated systems. The force-displacement characteristics of the spring-driven system is set by the spring stiffness, k. Given a fixed maximum force, $F_{\max}$, and range-of-motion, d, for the motor, the spring stiffness determines the amount of elastic energy the motor can store in the spring. The output of the spring-driven system is therefore sensitive to the inertia and stiffness of the spring, which ultimately depend on both the material properties and geometry of the spring.

To illustrate the effect of changing material properties of the spring, we performed a simulation of the spring-driven system in which the spring is assumed to be a uniform rod, storing and releasing elastic energy under uniaxial compression. The maximum kinetic energy of the spring-driven projectile depends on both the cross-sectional area and elastic modulus of the spring material (Fig. 4a), and is strongly dependent on how close the resulting spring stiffness is to the optimal stiffness set by the properties of the loading motor ($k_{\text{opt}} = F_{\max}/d$). Compared to the $F(x, v)$ relationship for the spring at optimal stiffness (Fig. 3b), using a spring that is either too compliant (Fig. 4b) or too stiff (Fig. 4c) reduces projectile velocity. Stiffness is a composite property that has both geometric and materials contributions; therefore, if a spring material with a low modulus is

used, a larger cross sectional area of the spring is required to reach k_{opt}. This requires a heavier spring and increases the inertial contribution of the spring, thus reducing the final kinetic energy achieved by the projectile (upper left of Fig. 4a).

Therefore, multiple factors influence the power capacity of a spring: the inertia of the driven mass, the spring's material properties, and the maximum recoil rate of the spring. The maximum recoil rate is presumably a function of both its inertial and material properties. When the driven mass is much greater than the mass of the spring, the recoil rate of the spring becomes insignificant. However, given that the greatest accelerations are produced by driving the smallest masses, spring-actuated systems are likely to operate in a realm in which limitations of the spring cannot be ignored. The limits on power amplification, therefore, depend on how fast springs can recoil and the forces that they generate during rapid recoil.

The challenges of measuring and making use of the force-velocity relationships of real springs

A practical, whole-system analysis of springs recoiling under the power of their own stored elastic energy would require the characterization of force-velocity relationships. Most dynamic material tests drive a material at a known strain rate and measure the resultant resistive force (44–52). Even though this approach reveals how spring properties change in dynamic conditions, these tests do not mimic the system's natural loading, and therefore do not reveal how the actual loading and unloading conditions influence the recoil dynamics of the spring. Although measuring material properties at rates comparable to the natural unloading rate of the spring presents a significant experimental challenge (53), for power amplified systems it is critical to understand ~~how~~ materials properties ~~of springs~~ influence ~~their~~ recoil rate when ~~they are~~ driving a small mass.

Insights into the recoil kinetics of compliant materials with simple geometries have come from studies of the free recoil of rubber and elastic bands (54–60). These studies have often relied upon visualization of material deformation for strain rate data collection, which is viable for large deformations of compliant materials, but difficult in small biological springs undergoing small-scale motions at high rates. Therefore, ~~new~~ techniques are needed to measure the maximum rates of

spring release under variable loading conditions and can address core questions, such as: What type of spring converts stored potential to kinetic energy most efficiently? What properties influence recoil time? Does a spring storing energy in bending recoil faster than one put in uniaxial extension? A more thorough understanding of material and geometric effects can inform the limits of spring recoil and unloading dynamics.

The material and geometric properties of biological springs are diverse (Table 2), yet it is not fully understood how their configurations influence recoil rate and elastic energy storage capacity. Biological springs are often monolithic with flexible and stiff regions distributed around a body or appendage segment. For example, mantis shrimp distribute both dense, stiff regions and thin, flexible regions around the appendage segment that dynamically flexes during spring loading and release (61). Other arthropod springs often consist of multiple materials (62–65), such as composites of structured stiff, high energy density materials bound within softer, resilient matrices (66–70). For example, the locust's leg combines the protein resilin with stiff cuticle to generate a flexible yet stiff spring (63); resilin provides resilience while the chitin nanofibers provide extensional stiffness required for a high energy density.

The integration of motors and springs has received some attention in biological systems, especially in terms of muscle-tendon dynamics. The relationship between the force capacity of a motor and the stiffness of a spring ultimately determines the amount of stored elastic energy (12, 71). This relationship is particularly important if the force capacity of the motor varies as a function of its length scale. Few studies have considered spring diversity, yet recent analyses point to multiple optima for spring stiffness depending on the temporal limitations set by the animal's behavioral use of the system (72).

Engineered systems use energy storage elements of various geometries and materials, including shaped polymer-fiber composites, SMA, molded elastomers, torsional and linear springs, and steel wires and ribbons (Table 2). Some engineered springs have been designed to store the maximum amount of energy given actuator or size constraints. For example, muscles do not have a Hookean force-displacement trade-off, so recurve bows are designed to flatten the force-displacement profile

of the spring to take advantage of the maximum force from muscle through a larger portion of the draw. To maximize stored energy density when driven by a DC motor, a tapered conical cross-section of elastomer was used to equalize shear stress throughout the spring for a jumping robot (73, 74). Other springs found in compound bows and jumping robots (28) have been designed with specific force-displacement profiles to delay peak acceleration. These systems typically incorporate a nonlinear spring within a more complex mechanism. Similar to the muscle-tendon system ~~above~~, some jumping robots use SMA for both actuation and energy storage to reduce size and weight of the integrated system (33, 34), decreasing the inertial component of their force-velocity trade-off.

Even though we have described the general categories of springs in both biological and engineered systems, the actual benefits in terms of power amplification and power density in these systems are simply not known. A key next step for both fields is to establish the mechanistic basis for and effects of springs as power amplifiers.

The role of latches

At a fundamental level, the role of latches is fairly obvious: the duration of latch release determines whether or not power amplification occurs. A short release time yields power amplification and a sufficiently long duration can completely eliminate power amplification. However, the central influence of latches in power amplification mechanisms extends far beyond the notion of the latch as a switch, or simple mechanism for energy release. Indeed, latches mediate the time, space, and rate over which potential energy is converted to kinetic energy (Fig. 5a). The latch's force capacity determines the maximum amount of stored energy, given the capacity of the underlying spring. The latch's shape and movement should influence the rate of the spring's delivery of force and velocity to the projectile, ~~but this dynamic interaction has yet to be studied~~. Therefore, ~~we focus this section's analyses on the following question:~~ *How do latches influence the dynamics of energy release?* Here we focus on latches that are simple mechanical structures with adjustable geometry (e.g., curvature) and dynamics (e.g., release velocity).

In the previous sections, our simulation used a latch with sharp edges which was removed at high velocity. This resulted in a nearly ideal latch, which releases energy instantaneously. By contrast, in this simulation, we incorporated latch duration, shape, force capacity, mass, and rate of energy release to test how these factors influence projectile kinematics. We found that the duration and kinematic profile of latch release are influenced by the latch's shape (Fig. 5b). We altered the shape of the latch by increasing the radius of curvature of its edges and reducing the speed of latch removal such that the spring could begin releasing energy before the latch was fully removed. The kinetic energy of the projectile was reduced due to both a change in the release point (there is more stored energy left in the spring when the latch force goes to zero for a smaller radius latch) and a change in the release velocity (constrained by the latch velocity and shape). The maximum kinetic energy of the projectile decreases as the latch deviates further from an ideal latch (Fig. 6), in terms of geometry and latch removal kinematics (larger corner radius of curvature and slower latch removal velocity). The properties of the latch can dramatically alter the $F(x,v)$ landscape of the spring-driven system (Fig. 6).

The diversity of biological and engineered latches

Even with many latch designs ~~and patents in engineering~~, and the diverse evolutionary ~~history of latching and~~ control in biology (Table 2) (75, 76), the relevant metrics and dynamics of latch performance are still in need of basic characterization and analysis. Latches can incorporate a range of physical forces, such as osmotic transitions, magnetics, and phase changes (76–78) (Tables 1,2). Biological latches use contact forces, geometric instability, pressure transitions, and cohesive forces (Table 2). For example, trap-jaw ants (Myrmicinae) remove a physical block to release their fast-rotating mandibles (79). Venus flytraps incorporate changes in turgor pressure that gradually alter the curvature of the leaves such that energy is suddenly released when the leaf geometry changes from convex to concave (80). Fern sporangia resist energy release with water pressure – sudden cavitation of the water triggers spore release (17). Similar in principle to the ferns, snapping shrimp use water cohesion to enable energy storage in the system until sufficient tension is generated and the cohesive forces are overcome (81). Ballistospores of the jelly fungus are launched at the instant

when two water surfaces coalesce and release surface tension energy. Grasshoppers use a lever arm system that generates a 'positive feedback' loop to trigger their jumps (82).

While most of the biological literature on latches is focused on their presence or general mechanism, the relationship between the energy release rate of a spring and the properties of the latch has been demonstrated as central to kinematic control in some systems. For example, several kinds of insects – fleas, froghoppers, and leafhoppers – rely on a well-tuned relationship between the latch linkages and the spring to minimize jerk. In these systems the linkage increases mechanical advantage of the spring at approximately the same rate that the force in the spring decreases, resulting in an approximately constant acceleration (64, 83).

Engineered systems also employ a wide variety of latches including disengagement of physical structures based on contact forces, geometric re-arrangements, and electromagnetic fields (Table 2). One of the oldest examples of a contact based force latch is a cam mechanism described in the 15th century by Leonardo da Vinci (84). This device uses intermittent contact to store potential energy in a slowly rising hammer, that generates a large impact when released. The common mousetrap is another example in which a contact latch (a latch formed by physical contact between two structures) releases the spring-loaded trap upon disengagement (85). The EPFL 7g robot is a modern design that utilizes the cam mechanism as a contact latch and releases the energy stored in torsional springs for efficiently jumping over large obstacles on rough terrains with small payloads (22). Inspired by jumping insects, the water strider jumping robot exploits a geometric latch and uses a torque reversal catapult (TRC) mechanism to take-off on both terrestrial and water surfaces (33). A Venus flytrap inspired system uses a different geometric latch that is based on snap-buckling instabilities in carbon fibre polymer composites that are actuated using shape memory alloys (SMA) (35). A chameleon tongue inspired system uses a coil gun (electromagnetic coils) to launch a permanent magnet connected to a elastomer to replicate projection, catching and retraction (86). In cases where engineered systems rely on chemical reactions to power their motions, an explicit latch may not be present (38, 87, 88).

Assessment and integration of power amplification mechanisms

Power amplification emerges from the integration of motors, springs, and latches. In biological systems, power amplification is calculated as the power output of the system relative to the maximum power output of the underlying muscle or, in a more conservative approach for systems in which muscle power output has not yet been quantified, relative to the highest measured power output of any biological system. Therefore, maximizing power amplification is achieved by reducing the power output of the motor and shifting the power performance of the system to the spring's dynamic properties. In addition, the latch and any additional linkages between the spring and the environment act to make this power delivery as effective as possible for a given task. The focal questions of this section are: *What does the calculation of power amplification reveal about performance and tuning? Are there general principles of integrated tuning for power-amplified systems?*

In our final series of results from the mathematical model, we demonstrate how changing the spring, latch, and motor properties influence power amplification. In most regards, these findings echo and strengthen the findings of the earlier sections, but they specifically emphasize that to achieve the greatest power amplification, it is not just enough to enhance the properties of the spring and match them to the motor, but it is also critical to shift the motor's properties away from maximal power output and instead toward maximal force output. The performance of the spring-driven system increases with motor force or motor range of motion, but does not depend on the maximum motor velocity. Therefore, increasing $F_{\max}$ or d (even at the expense of $v_{\max}$) would result in an increase in performance. However, if the other elements in the system (e.g., spring, latch) are fixed, increasing the motor force or motor range of motion does not necessarily lead to an increase in performance. The system needs to be fully integrated to confer the benefits of increasing the motor capabilities.

We illustrate this point using our model by allowing the maximum force output of the motor to increase (Fig. 7). If the spring stiffness is tuned to its optimal value as a function of $F_{\max}$, then the maximum kinetic energy of a spring-driven projectile monotonically increases as a function of $F_{\max}$ (Fig. 7a, solid curve), and power amplification intensifies (Fig. 7b, solid curve). On the other hand,

289 if the spring stiffness is fixed to the optimal stiffness for $F_{max} = 20\,N$, and, of equal importance, if
290 the motor has no increased range-of-motion or the position of the latch is fixed, then increasing
291 the maximum force capacity of the motor beyond 20 N does not result in any additional kinetic
292 energy delivered to the projectile (Fig. 7a, dashed curve), and power amplification is diminished
293 (Fig. 7b, dashed red curve). In other words, although a motor with a larger force capacity has the
294 potential capability to produce more energy, unless the spring can store that energy over the limited
295 range-of-motion of the motor, the motor will not reach its maximum force capacity and the overall
296 performance of the system will not improve. This coupling is important not only between the spring
297 and motor, but between all elements of the system including the latch.

298 ***Integration and evolution of existing power-amplified systems***

299 Biological power-amplified systems necessarily evolved together, yet engineering design often
300 struggles to achieve similarly tuned integration. However, given that both biological and engineered
301 systems operate under the same physical rules ~~that we have modeled simply in this paper~~, the
302 principles of integrating systems and synthetic design should ultimately emerge from these first-
303 principles analyses.

304 These challenges of integration can be addressed in terms of focused studies of the mechanics
305 of particular species or synthetic systems and by analyzing the large dataset expressed by millions
306 of years of evolutionary diversification. Analogous to the multitude of products that have emerged
307 from the tinkering of engineers over the ages, evolutionary diversification has yielded a large
308 dataset of mechanisms that work in a range of environmental conditions. Interdisciplinary teams of
309 biologists, physicists, and engineers are now making use of these datasets to measure how biological
310 systems have resolved inherent physical trade-offs across sizes and environments (89, 90). Similarly,
311 analyses of actuator, spring, and latch mechanisms in biological systems, both independently and as
312 integrated units, have the potential to reveal how the trade-offs inherent to integration have been
313 resolved.

314 The most in-depth analyses of the evolutionary dynamics of integrated biomechanical com-
315 ponents have been performed in the spring-driven, power-amplified system of mantis shrimp

(Stomatopoda). The motor, linkage system, spring, and tool (the actuated structure; in this case, a hammer or spear) of mantis shrimp have been analyzed as independent components and as a co-evolving mechanical system (91–95). Although latch evolution has yet to be considered, the spring and motor systems vary in concert across mantis shrimp. For example, when the extremely high acceleration hammering mantis shrimp evolved from the ancestral fish-spearing group, the muscles evolved force-modified architecture (up to 50 percent greater force generation at the cost of muscle contraction velocity when compared to spearers) and, with this shift in muscle force was an increase in spring work capacity (the springs of hammering shrimp perform greater work than the slower spearers).

The mantis shrimp's motor, spring, and tool evolved with varying degrees of integration (i.e., correlation among parts). Tighter integration over evolutionary time among these components is correlated with greater kinematics and spring function, but yet also incurred slower evolution in terms of rate and total accumulation of change. Put simply, the most powerful mantis shrimp have more tightly integrated components, but at the cost of evolvability. This trade-off between integration and evolvability may also be relevant to engineering design, given that retaining flexibility of design for different goals may bear a cost in terms of integration and performance.

~~Similar analyses could be performed on engineered systems to explore the history of power-amplified systems and also to adjust current designs for enhanced performance through better tuning.~~ In the history of power-amplified systems, even the materials available for elastic energy storage shifted the performance and function of engineered systems: today's slingshot was made possible due to the new incorporation and availability of rubber materials. The tuning of engineered jumpers has also been examined in some spring-driven systems, including a galago-inspired jumping robot (73). In this case, the effects of various configurations of motors, springs, and linkages were compared using a vertical jumping agility metric (a combination of jump height and frequency). The investigators analyzed the robot's performance when the motor and spring were in series, which enabled rapid leg repositioning for multiple jumps. For these series-elastic configurations, a linkage was used to modulate the power delivery from the spring to the ground (similar to the function

of the latch in our parallel spring-motor model). Even though the spring was not included in the optimization ((74, 96) are examples of spring optimization approaches), this study enabled the analysis of trade-offs between motor power density and linkage design for series elastic jumpers. Following from our analyses in the previous sections, an integrated design approach offers a generalized framework for achieving improved dynamics and scaling in engineered systems.

Conclusions and next steps

Power-amplified biological systems are of particular interest for cross-disciplinary research, because they achieve a trio of combined capabilities that exceed current engineering performance (Tables 1,2): (1) high accelerations that (2) can be continuously fueled through metabolic processes and (3) are used repeatedly with minimal performance degradation throughout the life of the organism. Even though engineers have struggled to design lightweight and long-running devices that can deliver high power output (Table 1), biological systems have been performing such feats for millions of years and using these systems for a myriad of functions including jumping, dispersal, impact fracture, and needle puncture (Table 1). Still, biological power-amplified systems are fundamentally limited in terms of size - they are universally small (Fig. 8; Tables 1,2) - while engineered systems far exceed the spatial scale depicted in Fig. 8.

Although we focused on a binary comparison in this paper - motor-driven v. spring-driven - many biological systems fall somewhere in the middle of this range. Elastic mechanisms in biology are used for a range of functions, including power attenuation, efficiency, and power amplification (6–11). Systems using motor-spring configurations to keep as much energy within the system (i.e., efficiency) are most often found in locomotor or running mechanisms (e.g., kangaroo hopping, human running). In contrast, the function of exclusively spring-driven systems, such as archery or mantis shrimp, is to direct as much energy in as short a time as possible into a target or structure, for puncture, fracture, jumping, or other high power tasks. As the relative contributions and trade-offs of the motor, spring, and latch are more fully explored and understood, scientists and engineers

will be able to resolve size-scaling constraints and explain how different combinations of these components can yield distinct functional uses.

This study demonstrates the rich potential for understanding, analyzing, and designing effective, integrated dynamics of power-amplified systems. We showed how the individual components of power-amplified systems and their interactions are essential to dynamic outputs and offer a greater potential for kinematic performance than has been previously recognized (although see (12)). Study of power-amplified systems provides a significant opportunity to establish fundamental principles of actuators, materials, and latches in their own right and in the context of their dynamic interactions. Researchers across the fields of mathematics, engineering, and biology are well-poised to resolve these ~~new and classic~~ challenges through advances in high speed imaging, materials testing and synthesis, integrated engineering design systems, and ~~new~~ biological discoveries.

Acknowledgments

We thank Leah Fitchett, Alex Guo, Martha Muñoz, Ryan Orszulik, and Ben Perlman for comments and assistance.

This material is based upon work supported by the U. S. Army Research Laboratory and the U. S. Army Research Office under contract/grant number W911NF-15-1-0358.

The data and analyses reported in this paper are presented in the Supplementary Materials.

Author contributions:

Conceptualization: all authors

Methodology: MI, SMC, AJC, XM, SB, SNP

Data collection/compilation: MSB, XM, SMC, YK, JSK, CYK, FZT

Revising/reviewing editing: all authors

Writing: MI, SMC, EZ, SB, SNP

Figures and Tables

Movement	System	Char. Length (m)	Mass (kg)	Duration (s)	Distance (m)	Max. speed ($m\,s^{-1}$)	Accel. ($m\,s^{-2}$)	Ref.
Biological Systems								
Nematocyst discharge	Hydra	1.0×10^{-5}	1.0×10^{-12}	1.0×10^{-6}	1.3×10^{-5}	3.7×10^{1}	5.3×10^{7}	(97)
Ballistospore ejection	Fungi	1.0×10^{-5}	3.7×10^{-13}*	1.0×10^{-5}	4.0×10^{-4}*	1.6	1.2×10^{5}	(13)
Pollen ejection	Bunchberry dogwood	1.0×10^{-3}	-	3.0×10^{-4}	-	3.6	2.4×10^{4}	(98)
Mandible strike	Trap-jaw ant	1.2×10^{-3}	7.0×10^{-8}	1.3×10^{-4}	-	6.7×10^{1}	1.6×10^{6}	(99)
Jump	Plant louse	1.9×10^{-3}	1.0×10^{-3}	4.0×10^{-4}	-	2.5	6.3×10^{3}	(100)
Suction trap	Aquatic bladderworts	2.0×10^{-3}	-	1.0×10^{-3}	-	1.5**	6.0×10^{3}**	(18)
Jump	Froghopper	6.1×10^{-3}	1.2×10^{-2}	8.8×10^{-4}	6.0×10^{-2}	4.7	5.4×10^{3}	(101)
Snap buckling	Venus flytrap	1.0×10^{-2}	-	1.0×10^{-1}	-	1.0×10^{-2}	1.0×10^{-1}*	(20)
Appendage strike	Mantis shrimp	1.0×10^{-2}	-	2.7×10^{-3}	-	2.3×10^{1}	1.0×10^{5}	(102)
Jump	Frog	4.5×10^{-2}	8.8×10^{-3}	8.1×10^{-2}	2.2	4.5	1.4×10^{2}	(103)
Tongue projection	Chameleon	4.7×10^{-2}	-	2.3×10^{-2}	1.2×10^{-1}	5.3	2.6×10^{3}	(104)
Jump	Locust	5.0×10^{-2}	1.7×10^{-3}	3.0×10^{-2}	3.0×10^{-2}	3.2	1.8×10^{2}	(105)
Escape maneuver	Northern pike	3.8×10^{-1}	4.5	8.5×10^{-2}	1.9×10^{-1}	4.7	1.6×10^{2}	(106)
Engineered Systems								
Jump	Micro elastomer jumper	4.0×10^{-3}	8.0×10^{-6}	6.0×10^{-1}	3.2×10^{-1}	3.0	6.0×10^{2}	(107)
Jump	Energetic silicon jumper	7.0×10^{-3}	3.1×10^{-4}	7.0×10^{-1}	8.0×10^{-1}	1.3	2.6×10^{2}	(38)
Jump	Water strider inspired robot	2.0×10^{-2}	6.8×10^{-5}	2.5×10^{-2}	1.4×10^{-1}	1.6	1.4×10^{2}	(33)
Projection	Chameleon tongue inspired sys.	2.0×10^{-2}	-	1.0×10^{-1}	1.6×10^{-1}	5.4	9.2×10^{2}	(86)
Jump	Flea inspired robot	3.0×10^{-2}	2.3×10^{-3}	5.0×10^{-1}	1.2	7.0	-	(108)
Jump	EPFL 7g robot	5.0×10^{-2}	7.0×10^{-3}	1.0	1.4	5.9	4.0×10^{2}	(22)
Jump	Steerable MSU jumper	6.5×10^{-2}	2.0×10^{-2}	-	5.5×10^{-1}	3.3	-	(109)
Jump	Soft combustion robot	3.0×10^{-1}	9.7×10^{-1}	1.1	7.6×10^{-1}	-	-	(87)
Jump	Locust inspired robot	1.4×10^{-1}	2.3×10^{-2}	2.0×10^{-2}	3.4	9.0	-	(32)
Catch	Flytrap inspired robot	1.5×10^{-1}	6.0×10^{-2}	4.0×10^{-1}	-	1.8	-	(35)
Jump	JPL hopper (2^{nd} gen.)	1.5×10^{-1}	1.3	3.0×10^{1}	9.0×10^{-1}	-	-	(28)
Jump	Galago inspired "Salto" robot	1.5×10^{-1}	1.0×10^{-1}	8.0×10^{-1}	1.0	1.8	-	(73)
Jump	Sandia Mars hopper	2.0×10^{-1}	5.0×10^{-1}	5.0	1.0	-	-	(88, 110)
Strike, catch	High-speed multifingered hand	3.0×10^{-1}	8.0×10^{-1}	3.2	-	4.5	-	(31)
Jump	Sand flea inspired robot	4.5×10^{-1}	5.0	-	8.0	-	-	(40)
Jump	Bipedal jumper "Mowgli"	9.0×10^{-1}	3.0	2.0×10^{-1}	5.0×10^{-1}	-	-	(39)

Table 1: **Biological systems exhibit a diversity of fast movements including jumps, projections, strikes and ejections at very small size scales, whereas the fast engineered locomotor systems are larger in size than biological systems and have been primarily designed for jumping movements.** The scaling and kinematics of a representative sample (not an exhaustive list) of fast biological and engineered movements are arranged by characteristic length scale. Characteristic length represents the size of the powered mass which can be the whole system (e.g. the body of jumping insects) or a part of it (e.g. the mandibles of trap-jaw ants, the stinging needle of nematocysts). In engineered systems, duration represents the total duration of motion, whereas in biological systems, duration is calculated only during acceleration. Biological movements operate in air (frog, grasshopper, Venus flytrap, trap-jaw ant, fungi, chameleon) or in aqueous environments (mantis shrimp, hydra, bladderworts, northern pike). However, all of the engineered systems listed here were designed for operation in air; note that the water strider robot jumps at the air-water interface. *estimated values from kinematic data reported, and **velocity and acceleration of fluid displaced by bladderwort trap.

Movement	System	Work input	Energy storage	Latch	Repeat.	Ref.
Biological Systems						
Appendage strike	Mantis shrimp	Muscle contraction	Exoskeleton	Contact	R-i	(102, 111)
Claw closure	Snapping shrimp	Muscle contraction	Exoskeleton	Fluidic (cohesion)	R-i	(81, 112)
Jump	Frog	Muscle contraction	Plantaris tendon	Geometric	R-i	(113, 114)
Jump	Grasshoppers, locusts	Muscle contraction	Resilin and chitin	Geometric	R-i	(62, 63)
Leaf closure	Venus flytrap	Turgor pressure	Cell wall	Geometric (instability)	R-i	(20)
Mandible closure	Trap-jaw ant	Muscle contraction	Exoskeleton	Contact	R-i	(79, 115)
Nematocyst discharge	Hydra	Osmotic gradient	Cell wall	Cohesion	NR	(97)
Spore ejection	Basidiomycota Fungi	Water condensation	Surface tension	Fluidic (coalescence)	NR	(13, 14)
Spore ejection	Fern sporangium	Dehydration	Annulus wall	Fluidic (pressure)	NR	(17)
Stalk contraction	Vorticella	Ionic gradient	Spasmoneme protein	Unkown	R-i	(116)
Tongue projection	Chameleon	Muscle contraction	Collagen sheaths	Contact	R-i	(117, 118)
Water suction	Bladderworts	Osmotic gradient	Trap wall	Geometric (instability)	R-i	(18)
Engineered Systems						
Catch	Flytrap inspired robot	SMA contraction	Bistable composite	Geometric (instability)	R-i	(35)
Jump	Micro elastomer jumper	Mechanical force	Elastomer	Contact	R-e	(107)
Jump	EPFL 7g robot	DC motor	Torsional spring	Contact	R-i	(22)
Jump	Steerable MSU jumper	DC motor	Torsional spring	Geometric	R-i	(109)
Jump	JPL hopper (2^{nd} gen.)	DC motor	Linear spring	Contact	R-i	(28)
Jump	Locust inspired robot	DC motor	Torsional spring	Contact	R-i	(32)
Jump	Galago inspired "Salto" robot	DC motor	Torsional spring	-	R-i	(73)
Jump	Water strider inspired robot	SMA contraction	SMA sheet, cantilever	Geometric (TRC)	R-e	(33)
Jump	Flea inspired robot	SMA contraction	SMA coil	Geometric (TRC)	R-e	(108)
Jump	Energetic silicon jumper	Chemical reaction	Nanoporous silicon	-	NR	(38)
Jump	Soft combustion robot	Chemical reaction	Combustion energy	-	R-e	(87)
Jump	Sandia Mars hopper	Chemical reaction	Combustion chamber	-	R-i	(88, 110)
Jump	Bipedal jumper "Mowgli"	Pneumatic actuator	-	-	R-i	(39)
Projection	Chameleon tongue inspired sys.	Coilgun	Capacitor	Electromagnetic	R-i	(86)
Strike	Mousetrap	Mechanical force	Torsional spring	Contact	R-e	(85)
Strike, catch	High-speed multifingered hand	DC motor	-	-	R-i	(31)

Table 2: **Biological and engineered systems exhibit diversity in the mechanisms of work input, elastic energy storage, latch mechanisms, and repeatability.** A repeatable system (R) can be used many times in contrast to a single-shot system (NR). The latch mechanisms are broadly categorized as: contact (resulting from physical contact between two structures), fluidic (mediated by microscopic and macroscopic fluid properties), geometric (dependent on changes in forces, moment arms and elastic instabilities due to geometrical configurations), and electromagnetic (arising from the interaction of electrically-charged particles). A final distinction among these systems is whether the system can repeat the motion without external manipulations (R-i) or whether they require external manipulation to prepare the system to fire again (R-e). Any repeatable biological system must be able to internally reset the system. However, many engineered systems still require an external device (or person) to reconfigure the system to the correct condition to fire again. Legends: SMA: shape memory alloy; DC: direct current, TRC: torque reversal catapult.

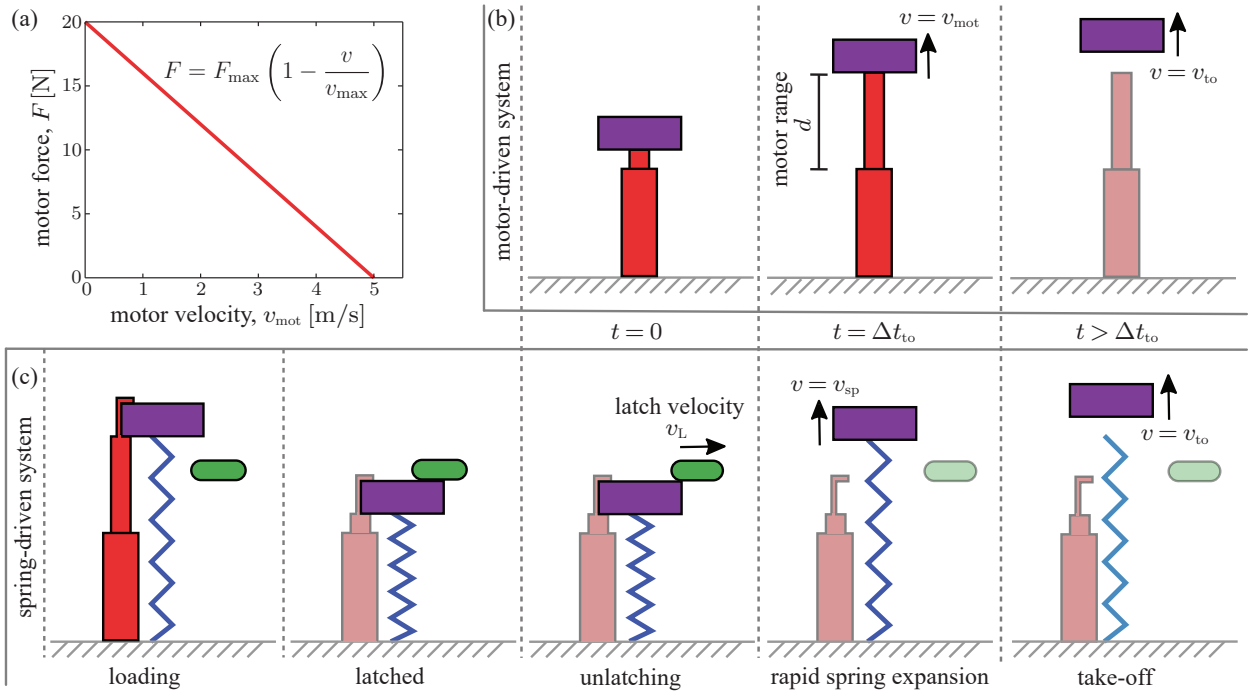

Figure 1: **Grounded in a linear force-velocity trade-off that operates in the same range of force and velocity as a biological motor, we mathematically modeled the factors influencing the power output of a projectile driven by either a motor or a spring (see Supplementary Materials for an analysis which includes dimensionless variables; see Glossary for variable definitions).** (a) This linear force-velocity trade-off approximates the output of a biological system and exhibits a maximum force (F_{max}) of 20 N and a maximum velocity (v_{max}) of 5 m/s. (b) Using the force-velocity relationship in (a), the motor (red) directly launched a projectile (purple) with velocity, v, equal to motor velocity (v_{mot}). At the instant that the projectile leaves the motor, the projectile's velocity was defined as its take-off velocity (v_{to}). The duration from initiation ($t = 0$) of projectile movement to its launch was defined as launch duration (Δt_{to}). The projectile's displacement, x, was defined such that $x(t = 0) \equiv 0$. (c) We used the same motor to load a spring (blue) that solely launched the projectile at the velocity of the spring ($v = v_{sp}$). We incorporated a latch (green) moving at velocity (v_L) to control the timing and release of elastic potential energy.

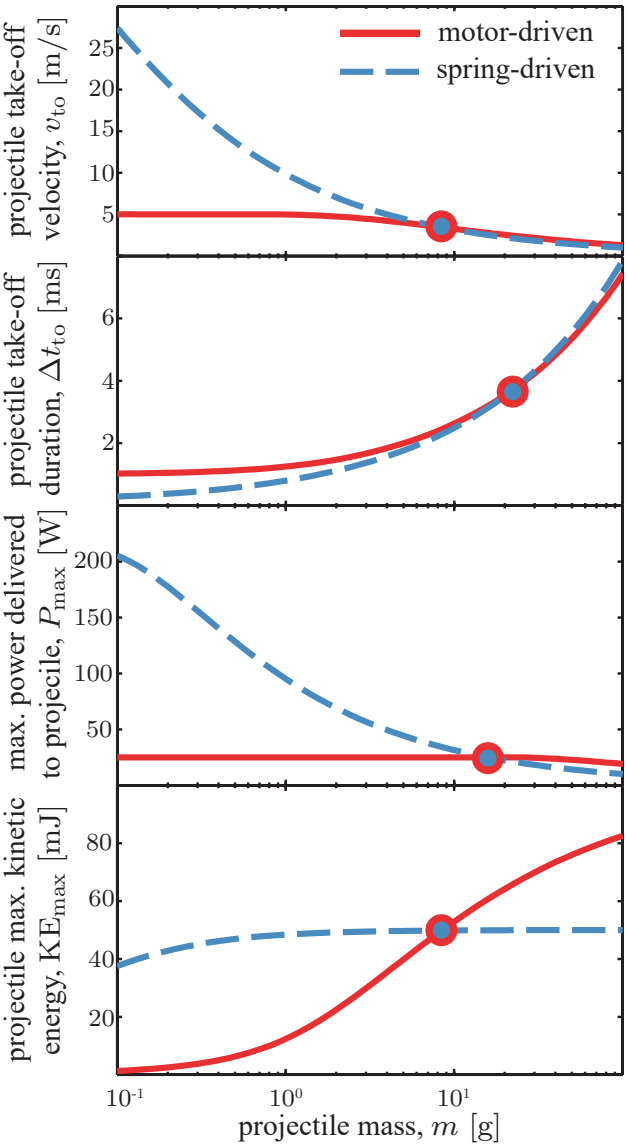

Figure 2: **Across a range of projectile sizes, a substantial transition occurs in projectile launch dynamics when motor-driven and spring-driven mechanisms are compared.** Using the motor-driven and spring-driven models pictured in Fig. 1, we simulated the launch of projectiles of varying mass, m (0.1-100 g), and calculated four parameters relevant to the kinematics of projectile launching: take-off velocity(v_{to}), take-off duration (Δt_{to}), maximal power output (P_{max}) and maximum kinetic energy (KE_{max}). Key transitions emerged in these parameters across the modeled size range of projectiles. At larger sizes, the motor-driven system performed moderately better than the spring-driven system. At smaller sizes, the spring-driven projectiles experienced substantial enhancements in kinetic energy, maximal power, and take-off velocity compared to motor-driven projectiles.

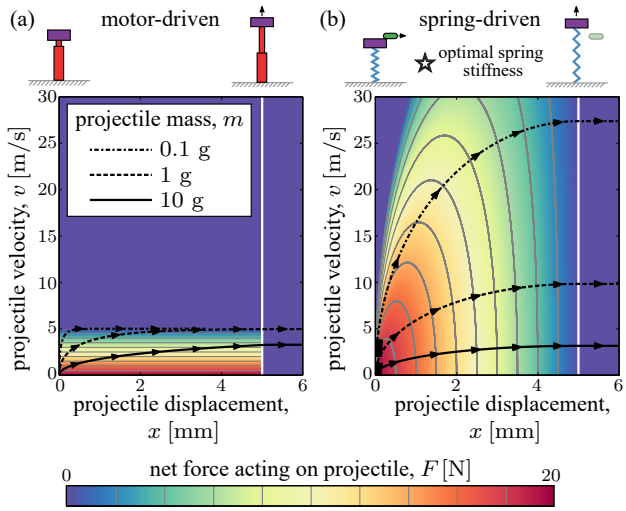

Figure 3: **The capacity for combined launching force and projectile velocity is greater in spring-driven than motor-driven systems, given similarly-sized projectiles.** The color contours indicate the net force of the motor or spring on the projectile and the black lines depict three examples of different projectile masses with their trajectories through x-v space (phase space). Take-off occurs when the projectiles reach the maximum displacement of the motor or spring at $x = d = 5$ mm (vertical white line). (a) Motor-driven projectiles, regardless of size, are constrained to take-off velocities below 5 m/s (see motor force-velocity constraints in Fig. 3). (b) Spring-driven projectiles, by contrast, encompass a roughly a 6-fold greater range of launch velocities than motor-driven projectiles, especially for small projectiles. The spring's force and velocity delivery was determined by a linear, Hookean relationship, but with the inertia of the spring included. Therefore, instead of vertical lines in phase space, which would represent a Hookean spring, the lines are curved to reflect the inertial effects of the spring's mass on its force-velocity behavior. The star symbol indicates that optimal spring stiffness was used in the simulation (see Fig. 4) and that the projectile was released using a latch with 0.2 mm radius of curvature (R) and removal velocity (v_{L}) of 5 m/s (see Fig. 5).

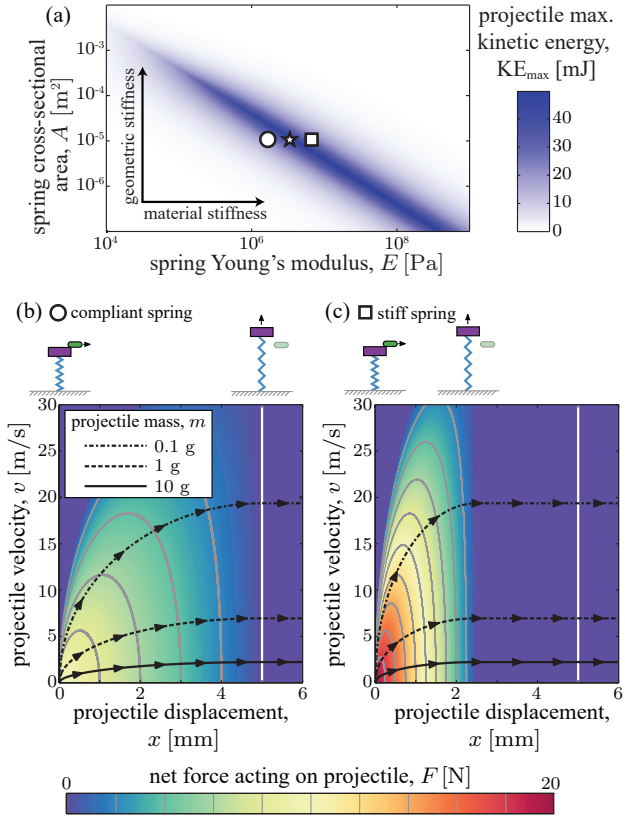

Figure 4: **Variation in spring properties substantially influences the force-velocity profile of projectile launching.** (a) By varying spring modulus and cross-sectional area, we simulated a distribution of the maximum kinetic energy of the projectile (KE_{max}). We applied the same motor and latch behavior as in previous simulations, varied the Young's modulus (E) and cross-sectional area (A) of the spring, while keeping spring length (L) and density (ρ) constant. Spring stiffness was calculated as $k = \frac{EA}{L}$. Spring cross-sectional area is a proxy for geometric stiffness and spring modulus serves as a proxy for material stiffness. Each symbol on the KE_{max} heat map corresponds to the projectile simulations in (b), (c), and Fig. 3. (b) A more compliant spring, ◯, yielded lower force, but similar projectile velocity when compared to (c) projectiles launched by a stiffer spring, □. The optimal spring stiffness for achieving maximal projectile velocity is depicted in Fig. 3, ☆.

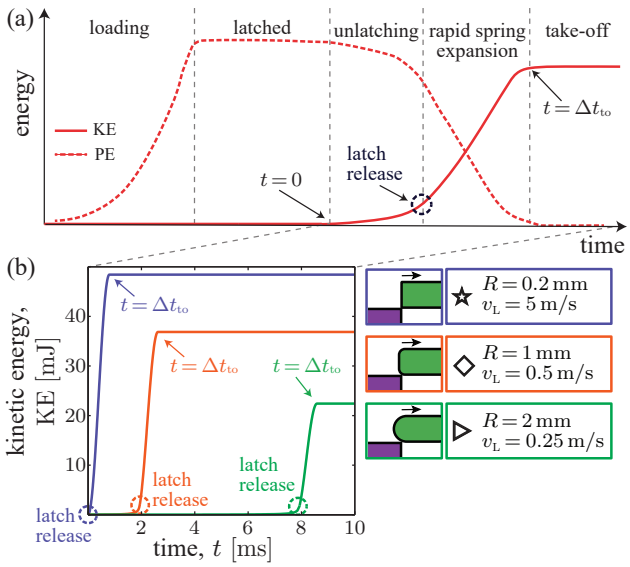

Figure 5: **The incorporation of a latch in spring-driven systems determines the timing, magnitude and rate of energy release.** (a) As the spring is loaded, potential energy (PE, dotted line) in the spring increases. The latch holds the loaded spring in place. Once the latch starts to release, PE decreases and kinetic energy (KE, solid line) increases until take-off when the projectile is completely free of the latch. (b) Projectile KE is strongly affected by the shape of the latches and their rate of removal. Three simulations applied different values for the latch corner radius (R) and latch removal velocity (v_L). Blue line, star: R=0.2 mm, $v_L = 5\,\mathrm{m/s}$. Red line, diamond: $R = 1\,\mathrm{mm}$, $v_L = 0.5\,\mathrm{m/s}$. Green line, triangle: $R = 2\,\mathrm{mm}$, $v_L = 0.25\,\mathrm{m/s}$.

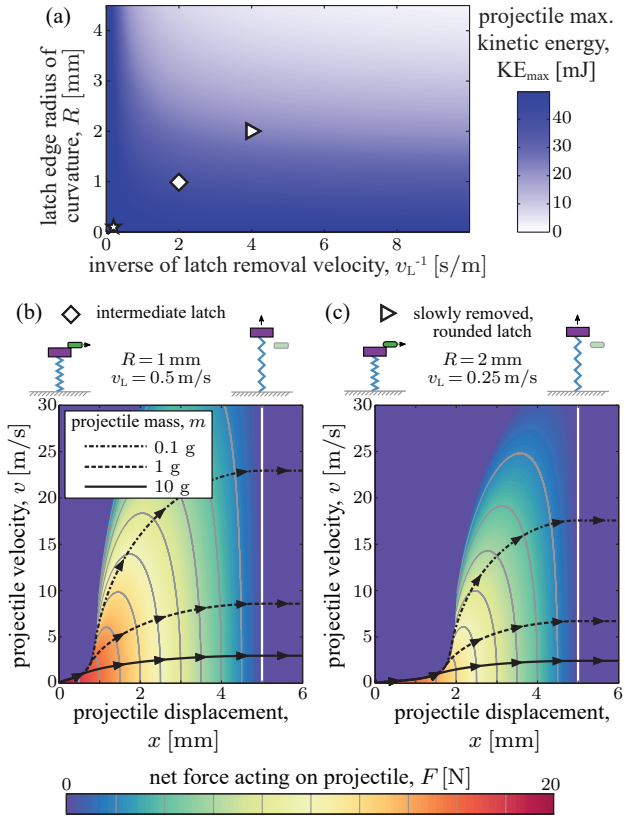

Figure 6: **Latch geometry and latch removal kinematics influence projectile kinetic energy and the force-velocity profile of spring-driven launches.** (a) The maximum kinetic energy of the projectile (KE_{max}) decreases as the latch's radius of curvature (R, see Fig. 6) is increased (star, $R = 0.2$ mm; diamond, $R = 1$ mm; triangle, $R = 2$ mm) and latch removal speed (v_L) is decreased (increased inverse latch removal speed, $1/v_L$). The star symbol refers to the simulation depicted in Fig. 3b to which both optimal latch and spring dynamics were applied. (b) This simulation applied the 1 mm radius of curvature latch at 0.5 m/s latch removal speed (diamond, Fig. 6) to a projectile launched with an ideal spring (Fig. 4). In this case, the force on the projectile was preserved and launch velocity remained high for small projectiles. (c) By contrast, the incorporation of a large radius of curvature (2 mm) and slower removal velocity (0.25 m/s) caused a substantial reduction in force development during launching which primarily affected the kinematics of smaller projectiles.

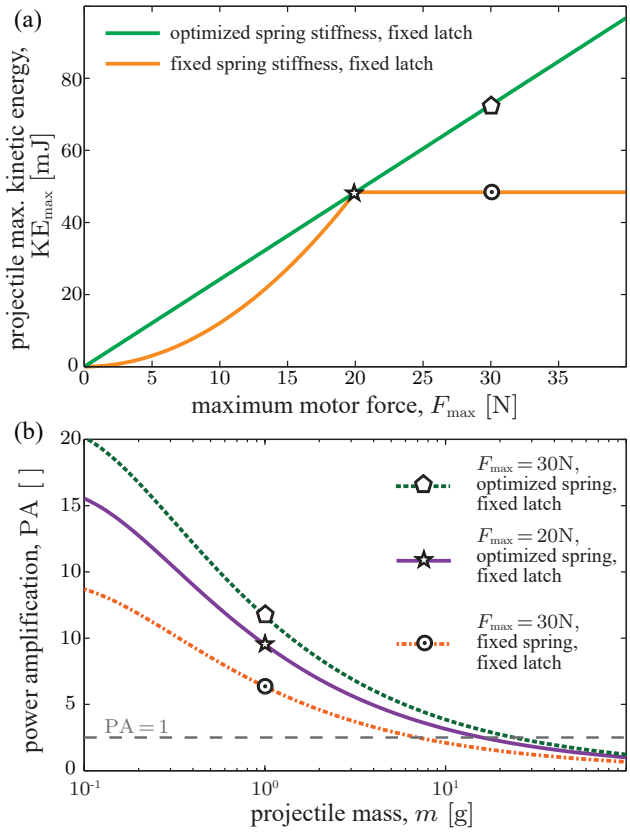

Figure 7: **The benefits conferred by the presence of springs and latches and by the strategic tuning of their properties ~~to the underlying motor's capabilities can be expressed in terms of power amplification and kinetic energy.~~** (a) The dependence of the maximum kinetic energy of a projectile on the motor force capacity is determined by whether the spring stiffness is optimized as a function of motor force (green line) or is fixed (orange line). This simulation was applied to a $m = 1$ g projectile. We simulated a motor with expanded force capacity compared to previous simulations (Fig. 1a), while keeping the motor range-of-motion fixed. Spring properties were optimized using the process illustrated in Fig. 4a. (b) Power amplification, PA (the ratio of maximum power delivered to the projectile from the spring-driven or motor-driven system), was strongly influenced by both the tuning of spring properties to motor properties as well as the projectile mass - particularly at smaller sizes. We simulated power amplification using earlier spring configurations (Fig. 7a) and again increased the force capacity of the motor. Tuning spring properties to motor force capacity enhanced power amplification beyond what could be achieved with a fixed spring stiffness, exemplifying the need to integrate and tune the motor, spring and projectile load when attempting to maximize the projectile kinematics.

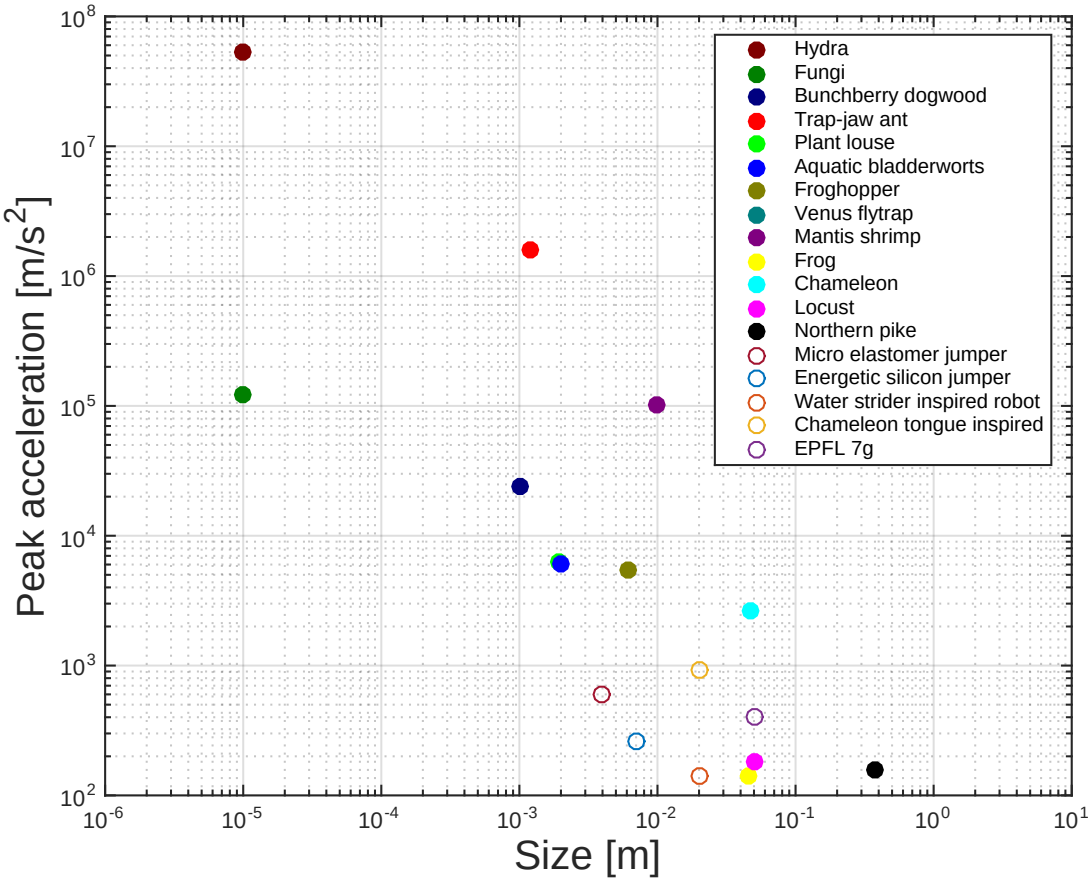

Figure 8: **~~When comparing~~ the fast movements of small engineered and biological systems, engineered jumpers (open circles) accelerate more slowly than biological systems (closed circles) when compared over a similar size range.** Engineered jumpers are several orders of magnitude larger than the smallest and highest performance of the biological systems. These data are from Table 1.

References

1. P. Aerts, *Philos. Trans. R. Soc. Lond. B. Biol. Sci.* **353**, 1607 (1998).

2. M. M. Peplowski, R. L. Marsh, *J. Exp. Biol.* **200**, 2861 (1997).

3. M. Burrows, *Nature* **424**, 509 (2003).

4. O. Barth, *Mechatronics* **10**, 545 (2000).

5. L. C. Rome, S. L. Lindstedt, *Physiology* **13**, 261 (1998).

6. T. J. Roberts, E. Azizi, *J. Exp. Biol.* **214**, 353 (2011).

7. S. N. Patek, D. M. Dudek, M. V. Rosario, *J. Exp. Biol.* **214**, 1973 (2011).

8. W. Gronenberg, *Journal of Comparative Physiology A* **178** (1996).

9. R. M. Alexander, H. C. Bennet-Clark, *Nature* **265**, 114 (1977).

10. R. M. Alexander, *Elastic Mechanisms in Animal Movement* (Cambridge University Press, 1988).

11. D. P. Ferris, M. Louie, C. T. Farley, *Proc. R. Soc. Lond., B, Biol. Sci.* **265**, 989 (1998).

12. A. Galantis, R. C. Woledge, *Proc. R. Soc. Lond., B, Biol. Sci.* **270**, 1493 (2003).

13. A. Pringle, S. N. Patek, M. Fischer, J. Stolze, N. P. Money, *Mycologia* **97**, 866 (2005).

14. X. Noblin, S. Yang, J. Dumais, *J. Exp. Biol.* **212**, 2835 (2009).

15. W. Gronenberg, B. Ehmer, *Zoology* **99** (1996).

16. M. M. Blanco, S. N. Patek, *Evolution* **68**, 1399 (2014).

17. X. Noblin, *et al.*, *Science* **335**, 1322 (2012).

18. O. Vincent, *et al.*, *Proc. R. Soc. Lond., B, Biol. Sci.* **278**, 2909 (2011).

19. J. M. Skotheim, L. Mahadevan, *Science* **308**, 1308 (2005).

20. Y. Forterre, J. M. Skotheim, J. Dumais, L. Mahadevan, *Nature* **433**, 421 (2005).

21. S. N. Patek, *Amer. Sci.* **103**, 330 (2015).

22. M. Kovac, M. Fuchs, A. Guignard, J.-C. Zufferey, D. Floreano, *IEEE International Conference on Robotics and Automation* (IEEE, 2008), pp. 373–378.

23. F. Li, *et al.*, *Mechatronics* **22**, 167 (2012).

24. J. Zhao, N. Xi, B. Gao, M. W. Mutka, L. Xiao, *IEEE International Conference on Robotics and Automation* (IEEE, 2011), pp. 4614–4619.

25. B. G. A. Lambrecht, A. D. Horchler, R. D. Quinn, *IEEE International Conference on Robotics and Automation* (IEEE, 2005), pp. 1240–1245.

26. S. A. Stoeter, P. E. Rybski, M. Gini, N. Papanikolopoulos, *IEEE/RSJ International Conference on Intelligent Robots and Systems* (2002), vol. 1, pp. 721–726 vol.1.

27. N. Fukamachi, H. Mochiyama, *IEEE International Conference on Advanced Intelligent Mechatronics* (2015).

28. J. Burdick, P. Fiorini, *The International Journal of Robotics Research* **22**, 653 (2003).

29. M. Kaneko, M. Higashimori, *Automation Congress,* (IEEE, 2004), pp. 117–122.

30. A. M. Johnson, D. E. Koditschek, *IEEE International Conference on Robotics and Automation* (IEEE, 2013), pp. 2568–2575.

31. A. Namiki, Y. Imai, M. Ishikawa, M. Kaneko, *IEEE/RSJ International Conference on Intelligent Robots and Systems* (IEEE, 2003), pp. 2666–2671.

32. V. Zaitsev, *et al.*, *Bioinspiration & Biomimetics* **10**, 066012 (2015).

33. J.-S. Koh, *et al.*, *Science* **349**, 517 (2015).

34. J.-s. Koh, S. Jung, R. J. Wood, K. Cho, *IEEE/RSJ International Conference on Intelligent Robots and Systems* (2013), pp. 3796–3801.

35. S.-W. Kim, *et al.*, *Bioinspiration & Biomimetics* **9**, 036004 (2014).

36. W. Lindsay, D. Teasdale, V. Milanovic, K. Pister, C. Fernandez-Pello, *Technical Digest MEMS 2001 14th IEEE International Conference on Micro Electro Mechanical Systems* (IEEE, 2001), pp. 606–610.

37. S. J. Apperson, *et al.*, *J. Propul. Power* **25**, 1086 (2012).

38. W. A. Churaman, L. J. Currano, C. J. Morris, *Journal of* ... **21**, 198 (2012).

39. R. Niiyama, A. Nagakubo, *Proceedings IEEE* (IEEE, 2007), pp. 2546–2551.

40. Bostondynamics Inc., Sandflea, http://www.bostondynamics.com/robot_sandflea.html.

41. H. Tsukagoshi, M. Sasaki, A. Kitagawa, T. Tanaka, *IEEE International Conference on Robotics and Automation* (IEEE, 2005), pp. 1276–1283.

42. F. E. Zajac, *Crit. Rev. Biomed. Eng.* **17**, 359 (1989).

43. T. J. Roberts, R. L. Marsh, *J. Exp. Biol.* **206**, 2567 (2003).

44. B. Hopkinson, *Phil. Trans. R. Soc. A* **213**, 437 (1914).

45. K. W. Hillier, H. Kolsky, *Proc. Phys. Soc. London, Sect. B* **62**, 111 (1949).

46. B. Justusson, M. Pankow, C. Heinrich, M. Rudolph, A. M. Waas, *Int. J. Impact Eng.* **58**, 55 (2013).

47. J. Yi, M. C. Boyce, G. F. Lee, E. Balizer, *Polymer* **47**, 319 (2006).

48. G. H. Staab, A. Gilat, *Exp. Mech.* **31**, 232 (1991).

455 49. M. Hudspeth, B. Claus, S. Dubelman, J. Black, *Rev. Sci. Instrum.* **84**, 025102 (2013).

456 50. A. D. Mulliken, M. C. Boyce, *Int. J. Solids Struct.* **43**, 1331 (2006).

457 51. C.-C. Chen, J.-Y. Chueh, H. Tseng, H.-M. Huang, S.-Y. Lee, *Biomaterials* **24**, 1167 (2003).

458 52. B. Wetzel, P. Rosso, F. Haupert, K. Friedrich, *Eng. Fract. Mech.* **73**, 2375 (2006).

459 53. C. R. Siviour, J. L. Jordan, *J. of Dyn. Behv. Materials* **2**, 15 (2016).

460 54. R. B. Bogoslovov, C. M. Roland, *J. Appl. Phys.* **102**, 063531 (2007).

461 55. P. H. Mott, *et al.*, *J. Polym. Sci., Part B: Polym. Phys.* **49**, 1195 (2011).

462 56. C. C. Lawrence, G. J. Lake, A. G. Thomas, *Int. J. Non Linear Mech.* **68**, 59 (2015).

463 57. J. G. Niemczura, On the response of rubbers at high strain rates., *Tech. rep.*, Sandia National
464 Laboratories (SNL), Albuquerque, NM, and Livermore, CA (United States) (2010).

465 58. R. Vermorel, N. Vandenberghe, E. Villermaux, *Phil. Trans. R. Soc. A* **463**, 641 (2007).

466 59. L. B. Tunnicliffe, A. G. Thomas, J. J. C. Busfield, *Polym. Test.* **47**, 36 (2015).

467 60. C. M. Roland, *Rubber Chem. Technol.* **79**, 429 (2006).

468 61. M. V. Rosario, S. N. Patek, *J. Morphol.* **276**, 1123 (2015).

469 62. M. Burrows, S. R. Shaw, G. P. Sutton, *BMC Biol.* **6**, 1 (2008).

470 63. M. Burrows, G. P. Sutton, *J. Exp. Biol.* **215**, 3501 (2012).

471 64. G. P. Sutton, M. Burrows, *J. Exp. Biol.* **214**, 836 (2011).

472 65. S. N. Patek, M. V. Rosario, J. R. A. Taylor, *J. Exp. Biol.* **216**, 1317 (2013).

473 66. J. F. V. Vincent, U. G. K. Wegst, *Arthropod Struct. Dev.* **33**, 187 (2004).

474 67. J. Gosline, *et al.*, *Philos. Trans. R. Soc. Lond. B. Biol. Sci.* **357**, 121 (2002).

475 68. D. Raabe, C. Sachs, P. Romano, *Acta Mater.* **53**, 4281 (2005).

476 69. J. F. V. Vincent, *Compos Part A Appl Sci Manuf* **33**, 1311 (2002).

477 70. D. Klocke, H. Schmitz, *Acta Biomater.* **7**, 2935 (2011).

478 71. D. Cofer, G. Cymbalyuk, W. J. Heitler, D. H. Edwards, *J. Exp. Biol.* **213**, 1060 (2010).

479 72. M. V. Rosario, G. P. Sutton, S. N. Patek, G. S. Sawicki, *Proc. R. Soc. Lond., B, Biol. Sci.* **283**,
480 20161561 (2016).

481 73. D. W. Haldane, M. M. Plecnik, J. K. Yim, R. S. Fearing, *Science Robotics* **1** (2016).

482 74. D. Rollinson, S. Ford, B. Brown, H. Choset, *Dynamic Systems and Control Conference.*
483 (ASME, 2013).

484 75. K. Kagaya, S. N. Patek, *J. Exp. Biol.* **219**, 319 (2016).

485 76. A. Sakes, *et al.*, *PLoS One* **11**, e0158277 (2016).

486 77. M. S. Rodgers, J. J. Allen, K. D. Meeks, B. D. Jensen, S. L. Miller, *Proceedings of the SPIE*
487 (1999), pp. 212–222.

488 78. R. E. Fischell, L. Wilson, *J Spacecr Rockets.* (1965).

489 79. W. Gronenberg, J. Tautz, B. Hölldobler, *Science* **262**, 561 (1993).

490 80. Y. Forterre, *J. Exp. Bot.* **64**, 4745 (2013).

491 81. R. Ritzmann, *Science* **181**, 459 (1973).

492 82. W. J. Heitler, *J. Comp. Physiol.* **89**, 93 (1974).

493 83. G. Bonsignori, *et al.*, *J. Exp. Biol.* **216**, 2161 (2013).

494 84. F. C. Moon, *The Machines of Leonardo Da Vinci and Franz Reuleaux*, Kinematics of Machines
495 from the Renaissance to the 20th Century (Springer Science & Business Media, 2007).

85. J. M. Keep, Animal Trap, Patent, US Patent Office (1879).

86. A. Debray, *Bioinspir. Biomim* **6**, 026002 (2011).

87. N. W. Bartlett, *et al.*, *Science* **349**, 161 (2015).

88. P. Weiss, *Sci. News* **159**, 88 (2001).

89. S. N. Patek, *Science* **345**, 1448 (2014).

90. G. K. Taylor, A. Thomas, *Evolutionary Biomechanics*, Selection, Phylogeny, and Constraint (Oxford University Press (UK), 2014).

91. M. M. Muñoz, P. S. L. Anderson, S. N. Patek, *Proc. R. Soc. Lond., B, Biol. Sci.* **284**, 2016325 (2017).

92. T. Claverie, E. Chan, S. N. Patek, *Evolution* **65**, 443 (2011).

93. T. Claverie, S. N. Patek, *Evolution* **67**, 3191 (2013).

94. P. S. L. Anderson, D. C. Smith, S. N. Patek, *Evol. Dev.* **18**, 171 (2016).

95. P. S. L. Anderson, S. N. Patek, *Proc. R. Soc. Lond., B, Biol. Sci.* **282**, 20143088 (2015).

96. J. Aguilar, A. Lesov, K. Wiesenfeld, D. I. Goldman, *Phys. Rev. Lett.* **109**, 1 (2012).

97. T. Nüchter, M. Benoit, U. Engel, S. Ozbek, T. W. Holstein, *Curr. Biol.* **16**, R316 (2006).

98. J. Edwards, D. Whitaker, S. Klionsky, M. J. Laskowski, *Nature* **435**, 164 (2005).

99. J. C. Spagna, *et al.*, *J. Exp. Biol.* **211**, 2358 (2008).

100. M. Burrows, *J. Exp. Biol.* **215**, 3612 (2012).

101. M. Burrows, *J. Exp. Biol.* **209**, 4607 (2006).

102. S. N. Patek, W. L. Korff, R. L. Caldwell, *Nature* **428**, 819 (2004).

516 103. R. S. James, R. S. Wilson, *Physiol. Biochem. Zool.* **81**, 176 (2015).

517 104. C. V. Anderson, *Sci. Rep.* **6**, 18625 (2016).

518 105. H. C. Bennet-Clark, *J. Exp. Biol.* **63**, 53 (1975).

519 106. D. G. Harper, R. W. Blake, *J. Exp. Biol.* **155**, 175 (1991).

520 107. A. P. Gerratt, S. Bergbreiter, *Smart Mater. Struct.* **22**, 014010 (2013).

521 108. J. S. Koh, S. P. Jung, M. Noh, S. W. Kim, K. J. Cho, *IEEE International Conference on*
522 *Robotics and Automation* (2013), pp. 26–31.

523 109. J. Zhao, J. Xu, B. Gao, N. Xi, F. J. Cintrón, *IEEE Trans. Rob.* **29**, 602 (2013).

524 110. J. German, *Sandia Lab News* **52** (2000).

525 111. T. I. Zack, T. Claverie, S. N. Patek, *J. Exp. Biol.* **212**, 4002 (2009).

526 112. M. Versluis, B. Schmitz, A. von der Heydt, D. Lohse, *Science* **289**, 2114 (2000).

527 113. H. C. Astley, T. J. Roberts, *Biol. Lett.* **8**, 386 (2011).

528 114. H. C. Astley, T. J. Roberts, *J. Exp. Biol.* **217**, 4372 (2014).

529 115. S. N. Patek, J. E. Baio, B. L. Fisher, A. V. Suarez, *Proc. Natl. Acad. Sci. U.S.A.* **103**, 12787
530 (2006).

531 116. L. Mahadevan, P. Matsudaira, *Science* **288**, 95 (2000).

532 117. J. H. de Groot, J. L. van Leeuwen, *Proc. R. Soc. Lond., B, Biol. Sci.* **271**, 761 (2004).

533 118. U. K. Müller, S. Kranenbarg, *Science* **304**, 217 (2004).

Supplementary Material

Supplementary Text

Table S1 and S2

Figs S1 to S12

Glossary

A Cross-sectional area of the spring material. 24

d Motor range-of-motion. 7, 13, 23

E Young's modulus of spring material. 24

$F(x, v)$ Force-displacement-velocity relationship: the net force acting on the projectile as a function of its displacement and velocity. 7, 11

F_{max} Maximum motor force. 7, 13, 14, 21

k Hookean spring constant. Defined by the length, cross-sectional area, and Young's modulus of the spring as $k = \frac{EA}{L}$. 7, 24

k_{opt} Optimum Hookean spring constant: defined by the motor properties as $k_{\text{opt}} = F_{\text{max}}/d$. 7, 8

KE kinetic energy. 25

KE_{max} Maximum kinetic energy reached by the projectile: defined by the projectile mass and take-off velocity as $\text{KE}_{\text{max}} = \frac{1}{2}mv_{\text{to}}^2$. 22, 24, 26

L Equilibrium length of the spring. 24

m Projectile mass. 4, 5, 22

554 m_s Mass of the spring: defined by the density, length, and cross-sectional area of the spring material
555 as $m_s = \rho LA$. 7

556 $P_{\max}$ Maximum power delivered to the projectile during its acceleration. 22

557 PA Power amplification: defined as the ratio of the maximum power output of the spring-driven to
558 the maximum power output of the motor-driven system driving a given projectile. 27

559 PE potential energy. 25

560 R Radius of curvature of the latch edge. 23, 25, 26

561 ρ Density of spring material. 24

562 SMA shape memory alloy. 6, 9, 10

563 Δt_{to} Projectile take-off duration: elapsed time from the start of motion until the moment the force
564 acting on the projectile falls to zero. 21, 22

565 v Projectile velocity. 21, 23

566 v_{L} Velocity at which the latch is removed from blocking the projectile. 21, 23, 25, 26

567 $v_{\max}$ Maximum motor velocity. 5, 13, 21

568 v_{mot} Motor velocity. 21

569 v_{sp} Velocity of spring during projectile launch. 21

570 v_{to} Projectile take-off velocity. 5, 21, 22

571 x Projectile displacement. 21, 23